Nano Energy 101 (2022) 107588

Contents lists available at ScienceDirect

Nano Energy

journal homepage: www.elsevier.com/locate/nanoen

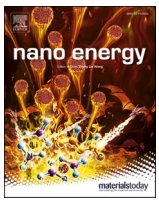

A stretchable and helically structured fiber nanogenerator for multifunctional electronic textiles

Fei Wu [a,b], Binxu Lan [a], Yin Cheng [a,*], Yi Zhou [c], Gaffar Hossain [d], Günter Grabher [e], Liangjing Shi [a], Ranran Wang [a,f,**], Jing Sun [a]

[a] State Key Laboratory of High Performance Ceramics and Superfine Microstructure Shanghai Institute of Ceramics Chinese Academy of Science, Shanghai 200050, PR China
[b] University of Chinese Academy of Sciences, Beijing 100049, PR China
[c] Department of Electrical and Computer Engineering, National University of Singapore, 4 Engineering Drive 3, Singapore 117583, Singapore
[d] V-Trion Textile Research GmbH, Schwefelbadstrasse 2a, 6845 Hohenems, Austria
[e] Grabher Group GmbH, Millennium Park 15, 6890 Lustenau, Austria
[f] School of Chemistry and Materials Science, Hangzhou Institute for Advanced Study, University of Chinese Academy of Sciences, 1 Sub-lane Xiangshan, Hangzhou 310024, China

ARTICLE INFO

Keywords:
Helical structure
Fiber nanogenerator
Energy harvesting
Motion sensing
Signal control

ABSTRACT

Fiber-based triboelectric nanogenerators (TENGs) possess advantages of good air permeability, excellent mechanical compliance, and easy integration into electronic textiles, and have wide application prospects in new-generation wearable electronics. However, few studies show the capability to unite favorable merits of excellent stretchability, high electrical generation, and conversion of multiple mechanical stimuli into a single fiber device. Here, we proposed a helically structured fiber-based triboelectric nanogenerator (HS-TENG) using $Ti_3C_2T_x$ as the triboelectric coating. The unique architecture endows the HS-TENG with large stretchability (~ 200 % strain), and high electric output (52 V, 1.5 μA, 4.2 μW) under compression for a 2 cm long device, superior to most stretchable triboelectric yarns. The HS-TENG also realizes multi-mode (i.e., stretch, press, twist, and bend) mechano-electrical conversion. The HS-TENG fiber can be integrated into electronic textiles (E-textiles) for versatile applications, including an insole for energy harvesting, a kneepad for motion sensing, and a glove for wireless signal control. This work provides new capabilities for multifunctional wearable systems.

1. Introduction

In recent years, wearable and multifunctional biomechanical sensors have aroused increasing attention due to their application potential in various fields such as healthcare, sports entertainment, and military defense [1–8]. However, their pervasive adoption in daily life is limited by the need to derive power from bulky and rigid batteries, as they not only reduce wearing comfort and portability, but also restrict the long-time outdoor service [9–15]. Therefore, a self-powered operation is highly desired in the design of wearable sensors for use in practical scenarios. Triboelectric nanogenerators (TENGs) represent a promising self-powered strategy for their high energy-harvesting efficiency, simple structure, design freedom in form-factor, and non-contamination to environments [5,16–20]. Highly conducting and electronegative TENG materials that support the generation of opposite triboelectric polarities and high currents are imperative for effectively harvesting electric power from biomechanical energy [21]. Among the family of electrically conducting materials, $Ti_3C_2T_x$ are triboelectrically more negative than poly tetrafluoroethylene (One of the most triboelectrically negative materials, which has been widely used in TENGs for achieving opposite triboelectric polarities [22]). Among different types of TENGs, fiber-based TENGs possess advantages of good air permeability, excellent mechanical compliance, outstanding fatigue resistance, and easy integration into electronic textiles [5,11,23–26]. These merits make fiber-based TENGs especially suitable for wearable electronics. Despite considerable progress in fiber-based TENGs [3,27–30], there still exist

* Corresponding author.
** Corresponding author at: State Key Laboratory of High Performance Ceramics and Superfine Microstructure Shanghai Institute of Ceramics Chinese Academy of Science, Shanghai 200050, PR China.
E-mail addresses: chengyin@mail.sic.ac.cn (Y. Cheng), wangranran@mail.sic.ac.cn (R. Wang).

https://doi.org/10.1016/j.nanoen.2022.107588
Received 14 April 2022; Received in revised form 27 June 2022; Accepted 8 July 2022
Available online 12 July 2022

limitations that hinder their extensive use.

One challenge is that the energy generation performance might decrease seriously due to large device deformation caused by human body movements (typically when exceed 30 % strain level): large strain can damage the electrode material and lead to permanent increase of electrical resistance [13,31–33]. This problem can be alleviated by selecting materials with good ductility and elaborate structural design [2,31,33–37]. For one thing, the ideal flexible electrodes are percolation networks composed of low dimensional conductive materials such as silver nanowires (AgNWs), carbon black, carbon nanotubes (CNTs) [34, 38–40]. To protect the fragile conductive networks, flexible polymers, such as polydimethylsiloxane (PDMS), poly tetrafluoroethylene (PTFE), and polymethyl methacrylate (PMMA), were exploited as encapsulating layer, which also served as the friction material [34,41–43]. However, the encapsulated electrodes are still unable to withstand large strains. For another, the fiber-based TENGs is usually designed as a structure with an inner core and an outer sheath [34,38,44]. A fiber-based conductive composite material with a coaxial structure reported by Dong et al. has high stretchability and excellent conductivity stability [32]. However, the energy harvested from human motion or surrounding environments (85 nW/cm^2 for a single fiber) is not high enough to power wearable electronics[45].

Another challenge is that most of these generators exhibited limited capability in harvesting multiple forms of mechanical energy (usually limited to pressing and bending), which inevitably led to waste of biomechanical energy [46–48]. Similarly, when such wearable generators were utilized for self-powered motion detection, their sensing range was frequently limited to a single type of human activity, due to the deficiency in sensing functionality [49–51]. With these concerns in mind, a wearable sensor for capturing various forms of mechanical stimuli, is particularly desirable.

To overcome these challenges, we proposed a flexible core-shell helically structured triboelectric nanogenerator (HS-TENG) using $Ti_3C_2T_x$ as the triboelectric coating. The unique core-shell helical structure enables the HS-TENG to not only maintain high power-generating performance (2.1 μW/cm) even under huge deformation (~ 200 % strain), but also succeed in converting multiple mechanical stimuli, including pressing, bending, stretching, and twisting, into electrical output. The electrical power can be easily scaled up by extending the length of the HS-TENG fiber: an open-circuit voltage of 160 V was achieved by pressing a meandering fiber of 10 cm in length, and lit up 165 commercial light-emitting diodes (LEDs). Such versatile HS-TENG fibers allow the convenient integration into smart electronic textiles (E-textiles). We demonstrated a series of HS-TENG enabled E-textiles, including a glove for signal control, a kneepad for motion sensing, and an insole for energy harvesting.

2. Results and discussion

As shown in Fig. 1a, we propose a novel helically structured triboelectric nanogenerator (HS-TENG). The HS-TENG consists of a core fiber with AgNW/$Ti_3C_2T_x$/PEDOT: PSS coating on the surface and a sandwiched Ecoflex/AgNW-fabric/Ecoflex helical outer sheath. The core fiber was selected as an elastic scaffold, composed of a highly elastic (up to 1077 % tensile strain, Fig. S1) polyurethane (PU) inner fiber and polyethylene terephthalate (PET) fibers winding around helically (Fig. S2). One reason to choose it is that the slippage of the woven PET layer during tensile deformation can accommodate the tensile strain, rather than direct stretch of PET fibers [52]. The good elastic resilience of this core fiber is validated by A multi-cycle load-unload test at a fixed strain of 120 % for 10 cycles (Fig. S3), which shows almost overlapped curves. Another is that the braided woven structure with increased specific surface area has good hygroscopicity. Therefore, the conductive materials (AgNWs and $Ti_3C_2T_x$) can be firmly adsorbed on the surface of the core fiber by a simple dip-coating method. The thickness of the conductive layer can be controlled by the concentration of the AgNW dispersion and dip-coating cycles. AgNWs were firstly adsorbed on the surface of the core fiber and formed a dense conductive network. It is

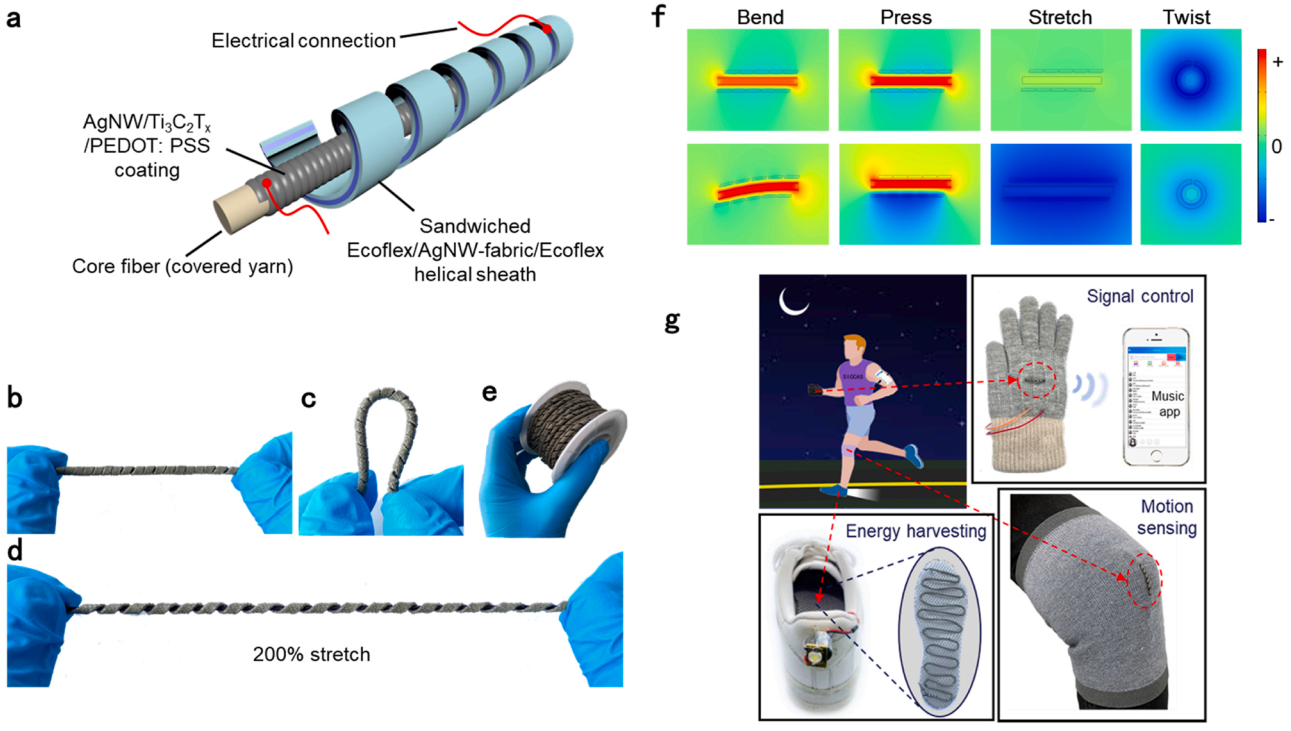

Fig. 1. The structure design and multifunctionality of the HS-TENG. (a) Schematic illustration of the structure of the HS-TENG. (b) Photograph images of the flexible HS-TENG, which can be (c) bent and (d) stretched to 200% tensile strain (e) The photograph of HS-TENG collected on reeling roller. (f) Simulation results of the electric potential distribution of different stimuli (bend, press, stretch, twist). (g) Application of HS-TENG based sensor in signal controlling, motion sensing, and energy harvesting.

believed that the selection of appropriate tribo-materials with opposite triboelectric polarities is crucial to achieving a high electrical output of TENGs [53–55]. For one thing, $Ti_3C_2T_x$ with a highly electronegative surface due to abundant surface terminations (–F, –OH, and/or ═O) was selected as the negative tribo-material, which was used to coat on the surface of the AgNWs [21,56,57]. And Poly(3, 4-ethylenedioxythiophene): poly (styrene sulfonate) (PEDOT: PSS) was added into the $Ti_3C_2T_x$ layer to promote the interface adhesion strength between the conductive layer and the PET fibers. For another, Ecoflex silicone rubber was selected as the positive tribo-material, which tends to lose electrons in contact with other materials [58]. Fig. S4 shows a photograph of the electrostatic voltmeter and the experimental setup for measuring the initial and after-contact surface potentials. The results of Ecoflex and $Ti_3C_2T_x$ after 20 cycles of contact-separation events are shown in Fig. S5. The sandwiched Ecoflex/AgNW-fabric/Ecoflex outer sheath was made by a strip of cotton elastic fabric with AgNW-coating as the electrode and covered by Ecoflex silicone rubber. To prepare the HS-TENG, the sandwiched outer sheath was helically wound around the core fiber (Fig. 1b). Based on the helical structure, the sensor exhibits excellent flexibility (Fig. 1c) and stretchability (up to 200 % tensile strain, Fig. 1d). In addition, this structure can be easily integrated, a twenty-meter length (not limited to this size) was fabricated shown in Fig. 1e. The rationale design of the core-sheath helical structure enabled the HS-TENG to transform various kinds of mechanical inputs into tribo-electrical signals. To further understand the spatial electric potential distribution of HS-TENG under various mechanical stimuli (e.g., bend, press, stretch, twist), we performed finite element analysis using COMSOL Multiphysics (Fig. 1f and Supplementary Note 1, Supporting information). The specific distribution of their electric potential is presented in Fig. S6. Interestingly, the electric potential varies significantly with variable gap distances between the two triboelectric dielectrics (Ecoflex and $Ti_3C_2T_x$). These results suggest that our proposed HS-TENG is applicable to multiple mechanical energy harvesting with desirable flexibility. Finally, such HS-TENG can be easily integrated into functional electronic textiles (E-textiles) for versatile applications, including an insole for energy harvesting, a kneepad for sports sensing, and a glove for signal control in music player (Fig. 1g).

Fig. 2a–c shows typical scanning electron microscopy (SEM) images of core fiber coated by AgNWs, $Ti_3C_2T_x$, and AgNWs/ $Ti_3C_2T_x$/ PEDOT: PSS respectively. AgNWs were coated tightly on the surface of core fiber to form a dense conductive network, as shown in Fig. 2a and Fig. S7a. This is because AgNWs with high aspect ratio have excellent flexibility, which makes them readily adsorbed on the surface of PET fibers [52]. As shown in Fig. 2b and Fig. S7b, $Ti_3C_2T_x$ nanosheets also can adapt to the woven structure of the fiber and tightly wrap the fiber surface. While the TENG coated by pure 2D materials often suffer from low stability and stretchability, which may be related with the low aspect ratio of 2D materials [56]. Therefore, we combined 1D material and 2D material to promote electrical conductivity and reduce the generation of cracks, which considerably improved the comprehensive performance of the HS-TENG. As shown in Fig. 2c and d, with the addition of 2D material — $Ti_3C_2T_x$, a leaf-like conductive network structure formed. We used AgNWs as leaf veins and the $Ti_3C_2T_x$ layer as leaf to wrap the surface of AgNWs to form a complete and continuous conductive path. To promote the interface adhesion strength between the conductive film and the PET fibers, we added PEDOT: PSS into the $Ti_3C_2T_x$ layer. More specifically, the morphological structure and the element analysis (EDS) of core fiber with AgNW/ $Ti_3C_2T_x$/ PEDOT: PSS coating were shown in Fig. S8–9. Fig. 2e is the cross-sectional SEM image of the prepared sandwiched Ecoflex/AgNW-fabric/Ecoflex outer sheath. The thickness of the Ecoflex layer in contacted with the core fiber with AgNW/$Ti_3C_2T_x$/PEDOT: PSS coating is approximately 110 μm. Fig. 2f shows the surface morphology of the AgNW-based elastic fabric. As shown in Fig. 2h, AgNWs are on the surface of the braided-woven-structured fabric. The braided woven

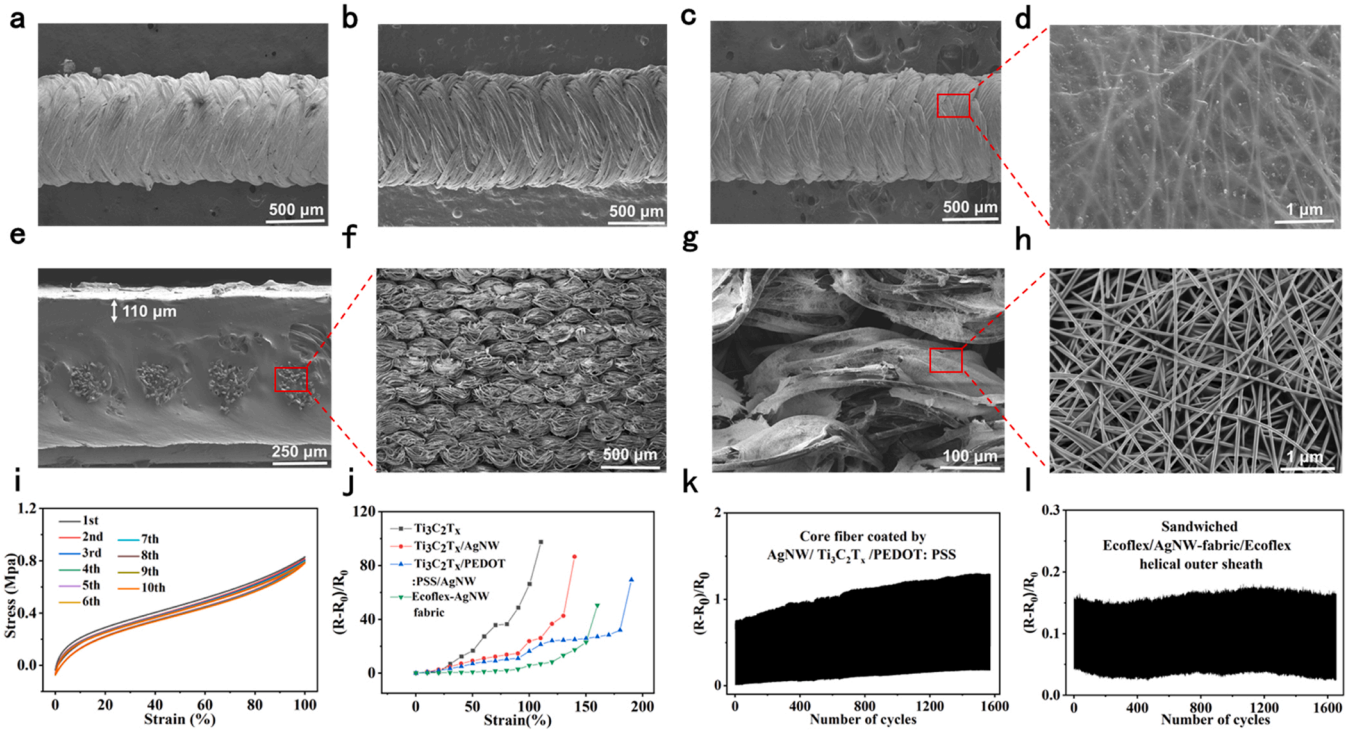

Fig. 2. Morphology and electromechanical characterization of HS-TENG. (a) SEM image of the core fiber coated by AgNWs. (b) SEM image of the core fiber coated by $Ti_3C_2T_x$. c, d) Low- and high-resolution SEM images of core fibers coated by AgNW/ $Ti_3C_2T_x$/ PEDOT: PSS. (e) Cross-section of the sandwiched Ecoflex/AgNW-fabric/ Ecoflex outer sheath. (f-g) Low- and high-resolution SEM images of the braided woven structure of AgNW-based elastic fabric. (h) AgNWs on the elastic fabric. (i) Stress-strain curves of the HS-TENG for continuous 10 cycles. (j) Relative resistance-strain curves of the sandwiched Ecoflex/AgNW-fabric/Ecoflex outer sheath and the core fiber coated by $Ti_3C_2T_x$, AgNW/$Ti_3C_2T_x$, and AgNW/$Ti_3C_2T_x$/PEDOT: PSS. (k) Durability testing of the core fiber coated by AgNW/$Ti_3C_2T_x$/PEDOT: PSS at a fixed strain of 50 %. (l) Durability testing of the sandwiched Ecoflex/AgNW-fabric/Ecoflex helical outer sheath at a fixed strain of 50 %.

structure of the cotton elastic fabric is beneficial to the adsorption of the AgNW dispersion and can reduce the damage to the conductive network under strain. The good elastic recovery of the HS-TENG is validated by the cyclic stretch-release tests at a fixed strain of 100 % for 10 cycles (Fig. 2i), which shows almost overlapped curves after the first cycle. As shown in Fig. 2j, by testing the relative resistance changes of core fibers coated by different components under strain, we compared the effects of the addition of AgNWs and PEDOT: PSS on the electromechanical properties of the $Ti_3C_2T_x$ composite core fibers. The resistances of core fibers coated by $Ti_3C_2T_x$, AgNW /$Ti_3C_2T_x$, and AgNW/ $Ti_3C_2T_x$ /PEDOT: PSS are about 800, 10, and 3 Ω/cm respectively. Fig. 2j shows the resistance of the core fiber with $Ti_3C_2T_x$ coating increases rapidly under tensile strain. Due to the low initial conductivity, it will adversely affect the output performance of the HS-TENG. In contrast, combining $Ti_3C_2T_x$ with PEDOT: PSS and AgNWs can not only improve the conductivity of the fiber but also enhance the interface bonding strength between the conductive materials and the scaffold fiber during the stretching process. Therefore, under stretch, the change of relative resistance of the core fiber with AgNW/$Ti_3C_2T_x$/PEDOT: PSS coating is slight. Finally, the durability of the core fiber coated by AgNW/$Ti_3C_2T_x$/PEDOT: PSS and sandwiched Ecoflex/AgNW-fabric/Ecoflex helical outer sheath was tested by 1500 cycles at a frequency of 1 Hz. Fig. 2k and l show just small fluctuations (increased by 1.5 and 0.15 respectively) in the resistance change of them during the 50 % stretching process, demonstrating the potential for long-term application.

Fig. 3a is the schematic diagram of the working principle of the HS-TENG under pressing, based on the dual mechanism of contact electrification and electrostatic induction, operating in a contact-separation mode. When the HS-TENG is pressed to result in the contact of the core fiber and sheath layer, $Ti_3C_2T_x$ layer and Ecoflex layer will be charged due to their different electron affinity. When the compression is released, electrons will flow from the inner electrode to the outer electrode to balance the generated triboelectric potential and will flow back to create a reverse current when the external force occurs again. An alternating current will be generated in the external circuit through the periodic contact-separation motion. It can be seen from the mechanism that the electronic performance of the HS-TENG is influenced by factors such as contact area, pressure, strain, and frequency. To characterize the energy-generating capacity of the HS-TENG, the open-circuit voltage (V_{OC}), short-circuit current (I_{SC}) and short-circuit charge transfer (Q_{SC}) are measured. We prepared a HS-TENG with a diameter of 3 mm and studied the influence of compression frequency, hybrid nanowire-nanosheet (AgNW-$Ti_3C_2T_x$) conductive network, and $Ti_3C_2T_x$ tribolayer on its electrical performance. The V_{OC}, I_{SC} and Q_{SC} generated by the HS-TENG under pressing increase with the increase of the compression frequency. When the compression frequency rises from 1 Hz to 3 Hz, the V_{OC}, I_{SC} and Q_{SC} increase from 15 V, 0.55 μA, and 9 nC to 52 V, 1.5 μA, and 12.5 nC respectively, which is superior to most of reported works on fiber-based TENGs (Fig. 3b–c and Fig. S10–11). In Fig. S12, the V_{OC}, I_{SC}, and Q_{SC} of $Ti_3C_2T_x$/PEDOT: PSS-based HS-TENG

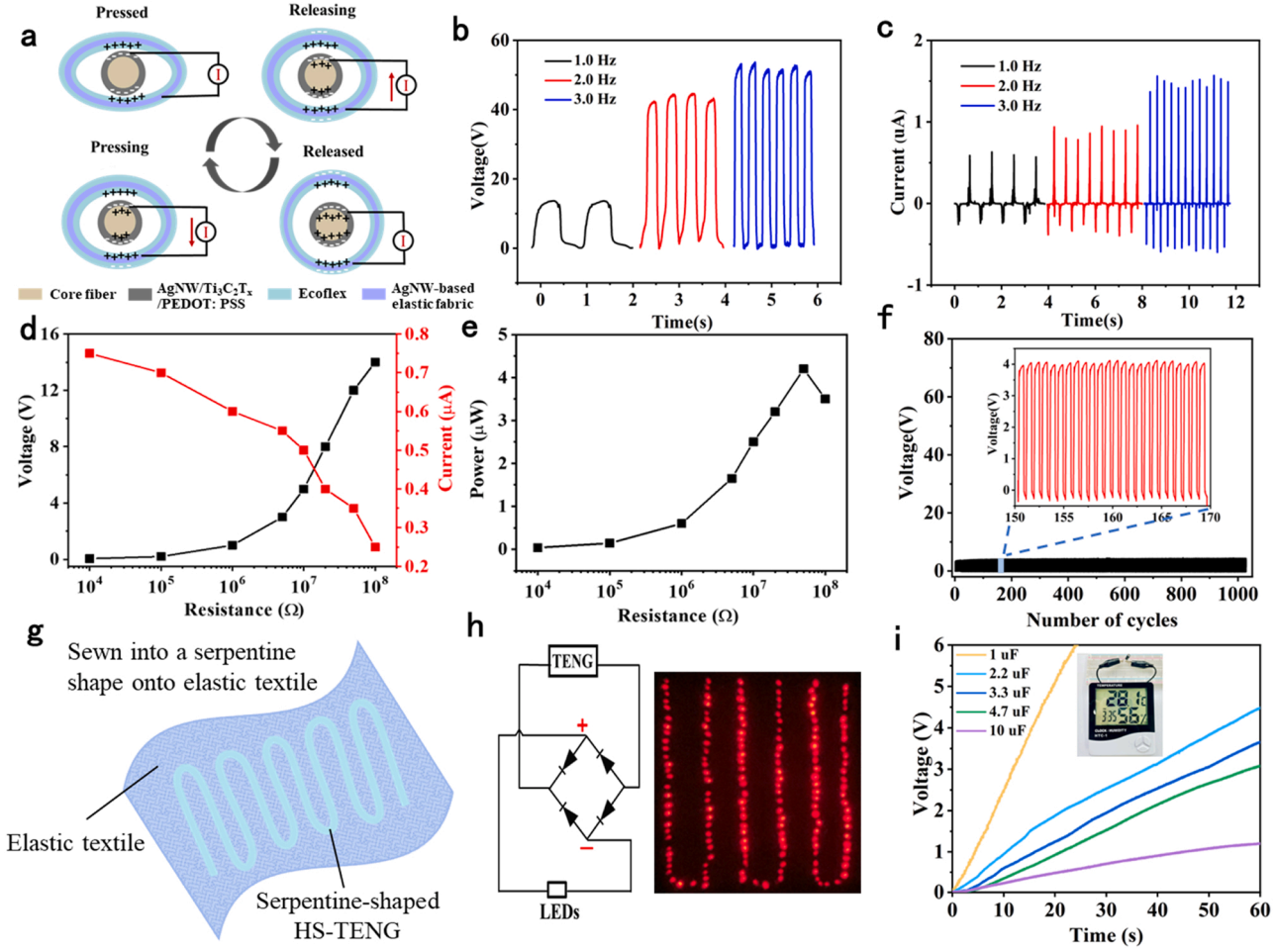

Fig. 3. Energy generation mechanism and the electrical output performance under pressing mode. (a) Schematic illustration of the working principle of the HS-TENG. (b) V_{OC} and (c) I_{SC} of the HS-TENG under different frequencies (1–3 Hz). (d) The variation of V_{OC}, I_{SC} and (e) power density of the HS-TENG with different external load resistance. (f) Durability testing of HS-TENG for continuous 1000 cycles. (Inset: the corresponding real-time V_{OC}). (g) Schematic illustration of a HS-TENG (length of 10 cm) integrated into an elastic textile. (h) the corresponding working circuit diagram (left) and lighting 165 red LEDs (right). (i) Charging curves of various capacitors by the HS-TENG (inset: the photograph of an electronic thermometer & hygrometer powered by the HS-TENG).

with a length of 2 cm under 3 Hz was 16 V, 0.4 μA, and 4.5 nC respectively, which was significantly lower than that of AgNW /$Ti_3C_2T_x$/PEDOT: PSS-based HS-TENG. It shows that the hybrid AgNW-$Ti_3C_2T_x$ percolation network not only help to promote the electromechanical property, but also is of benefit to energy generation performance of the HS-TENG. It may be due to that the dense conductive network formed by AgNW/$Ti_3C_2T_x$ is more conducive to the charge transfer. Compared with AgNW /$Ti_3C_2T_x$/PEDOT: PSS-based HS-TENG, the AgNW /PEDOT: PSS-based HS-TENG has a relatively low electricity output (5.6 V, 90 nA, and 1.4 nC 3 Hz) in Fig. S13, which shows the remarkable ability of $Ti_3C_2T_x$ tribo-layer to attracts triboelectrically generated electrons due to electronegative surface groups (T_x). The diameter of the core fiber can be selected as demand, and the output performance of the HS-TENG with a diameter of 1 mm is shown in the Fig. S14. The amplitude of the I_{SC} increase is higher than the V_{OC} and Q_{SC}. This is because the higher deformation rate leads to a higher flow rate of charges between two triboelectric layers, resulting in a higher current generation [35]. The power density is also measured by connecting different loads externally from 10 kΩ to 100 MΩ under the pressing frequency of 1 Hz. As displayed in Fig. 3d, as the load resistance increased from 10 kΩ to 100 MΩ, the V_{OC} increased while the I_{SC} decreased. The maximum output power density is 4.2 μW at a load resistance of 50 MΩ (Fig. 3e). The durability of the HS-TENG was also measured at a frequency of 1 Hz. As shown in Fig. 3f, the V_{OC} remains almost a constant of 4 V after 1000 contact-separation cycles, indicating excellent mechanical robustness and reliability. As shown in Fig. S15a, after 20 days of storage, the resistance of the electrode increased from 2.6 Ω/cm to 3.4 Ω/cm. Due to the high internal impedance of the TENG, the increase in the resistance of AgNW/ $Ti_3C_2T_x$ /PEDOT: PSS is acceptable, which has a negligible negative impact on the performance of the TENG [59]. As shown in Fig. S15b–d, the output performance of HS-TENG decreased by 30 % (from 13 V, 0.5 μA, 9 nC to 10 V, 0.35 μA, 6.5 nC). This may be due to the oxidation of surface terminations (–OH) of the $Ti_3C_2T_x$ [60], which adversely affects the electrical output performance of the HS-TENG. Moreover, machine washability is also a basic requirement for textiles in their actual application. The Fig. S16 demonstrates the washing environment and washing durability tests of our HS-TENG. The electrical output of the HS-TENG shows no significant degradation after 10 times washing (detailed information about washing condition and process in Supplementary Note 2, Supporting information).

To efficiently drive commercial electronics, we fabricated a HS-TENG with the length of 10 centimeters (Fig. 3g). Our HS-TENG can perform as a sustainable power source owing to its high electrical outputs (160 V, 8 μA, 45 nC Fig. S17). The Fig. 3h (left) demonstrates the corresponding circuit diagram of a self-powered system including the HS-TENG as a power source, a capacitor as an energy storage unit, and a rectifier (2W04, ASEMI) as an alternating current-to-direct current converter. Fig. 3h(right) shows HS-TENG can directly light up 165 red LEDs (Movie S1 in Supporting information). The charging curves of capacitors (1, 2.2, 3.3, 4.7, and 10 μF) by the HS-TENG are presented in Fig. 3i. The capacitor of 1, 2.2, and 3.3 μF can be rapidly charged to 3 V within 10, 40, and 55 s respectively. The illustration shows that the self-powered system integrated with HS-TENG and 10 μF capacitor can drive an electrical thermometer & hygrometer. The results show our HS-TENG is very promising as an efficient and clean power source.

Supplementary material related to this article can be found online at doi:10.1016/j.nanoen.2022.107588.

In addition to the compression, mechanical energy harvesting capability of the HS-TENG was also tested under bending, twisting, and stretching to investigate diverse working conditions. Fig. 4a–d illustrates the sensor under mechanical stimuli of bend, twist, stretch, and press. As shown in Fig. 4e, the V_{OC} increases distinctly from 0.35 V to 1.75 V when the extent of bending deflection changes from 0.5 cm to 2.0 cm. Similarly, when our HS-TENG is twisted from 30° to 270°, the V_{OC} increases from 0.15 V to 0.75 V (Fig. 4f). Moreover, when the stretch strain raises from 30 % to 120 %, the HS-TENG reveals an obvious enhancement in V_{OC} from 0.15 V to 1.2 V (Fig. 4g). The structure of the HS-TENG can provide adequate contact-separation operation space. The gap size between the inner core and the outer sheath will decrease gradually under diverse mechanical stimuli, thus contributing to

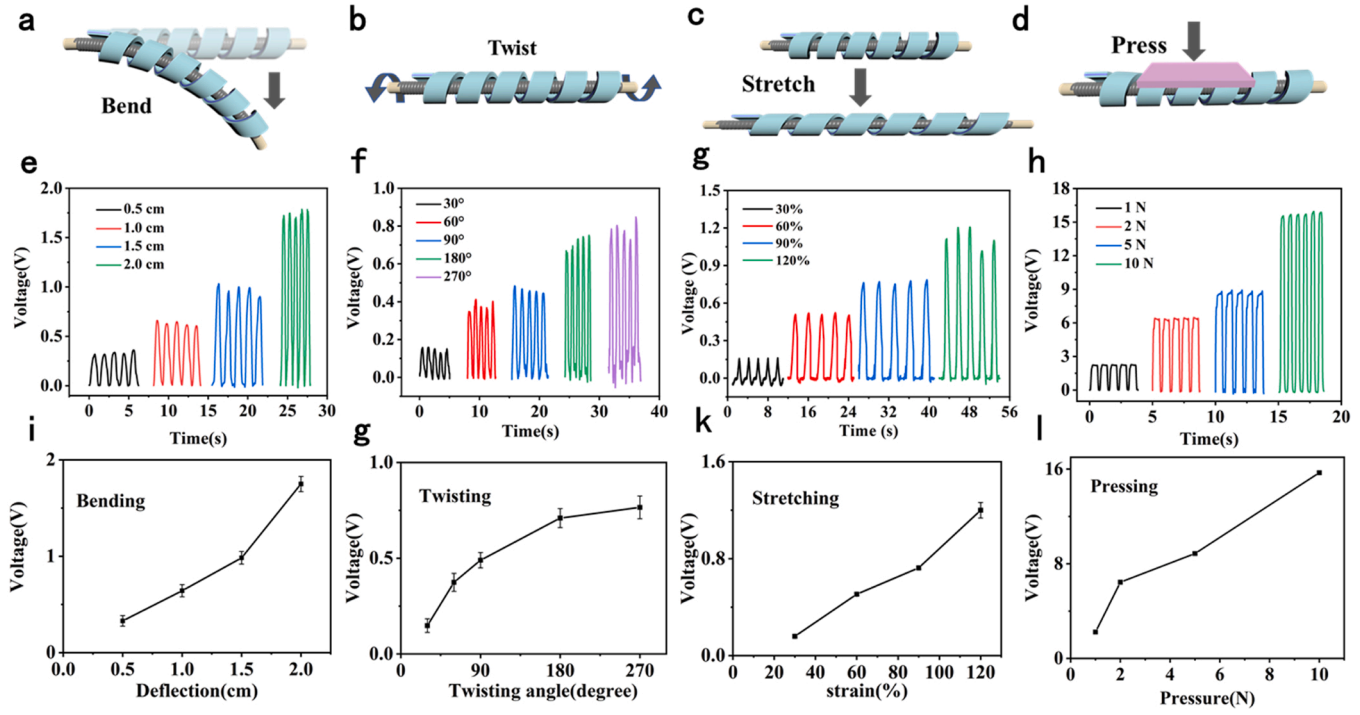

Fig. 4. Versatile mechano-electrical conversion of the HS-TENG. (a-d) Illustrations of the HS-TENG device under different mechanical stimuli. (e-h) Cyclic testing of HS-TENG for bending, twisting, stretching, and pressing. (i-l) The V_{OC} of the HS-TENG under mechanical input of bending (deflection of 0–2 cm), twisting (angle of 0–270°), stretching (a strain of 0–120 %) and pressing (force of 0–10 N).

obvious output signal. The V_{OC} of the HS-TENG under the compressing is much higher than those under other mechanical stimuli because the compressing operation may result in a much higher extent of gap size shrinkage. Another reason is that in pressing mode, the contact area between the inner core and outer sheath will be larger, and the tight squeeze is more conducive to contact electrification and electrons transfer Energy conversion under diverse deformations not only endow our HS-TENG with efficient mechanical energy harvesting ability, but also help to achieve sensing of various kinds of motions.

With high sensitivity response to a variety of mechanical stimuli, lightweight, flexibility, and stretchability, the HS-TENG is particularly suitable for energy harvesting, motion monitoring, and signal control (Fig. 5a). Collecting mechanical energy from runners enables the HS-TENG to be used as a self-powered lighting device during night running. The self-powered night-running light system consists of four main functional units: the HS-TENG (length of 80 cm) integrated into the insole, a full-wave diode bridge that rectifies the power output generated by the sensor, a 10 μF capacitor that can temporarily store the power output, and a commercial LED. First, the HS-TENG collects biomechanical energy from human motion and converts it into electrical energy. Then, the power output can directly illuminate the commercial LED, thereby acting as a safety warning during night-running (Movie S2 in Supporting information). Fig. 5b demonstrates the equivalent circuit (left) and the image (right) of a runner equipped with HS-TENG based self-powered night-running warning system. In terms of motion sensing, most human motions are related to joint bending and are accompanied by changes in the strain of the surrounding skin [61,62]. Through the stretch/bend sensing modes of the HS-TENG, the related motion of joint

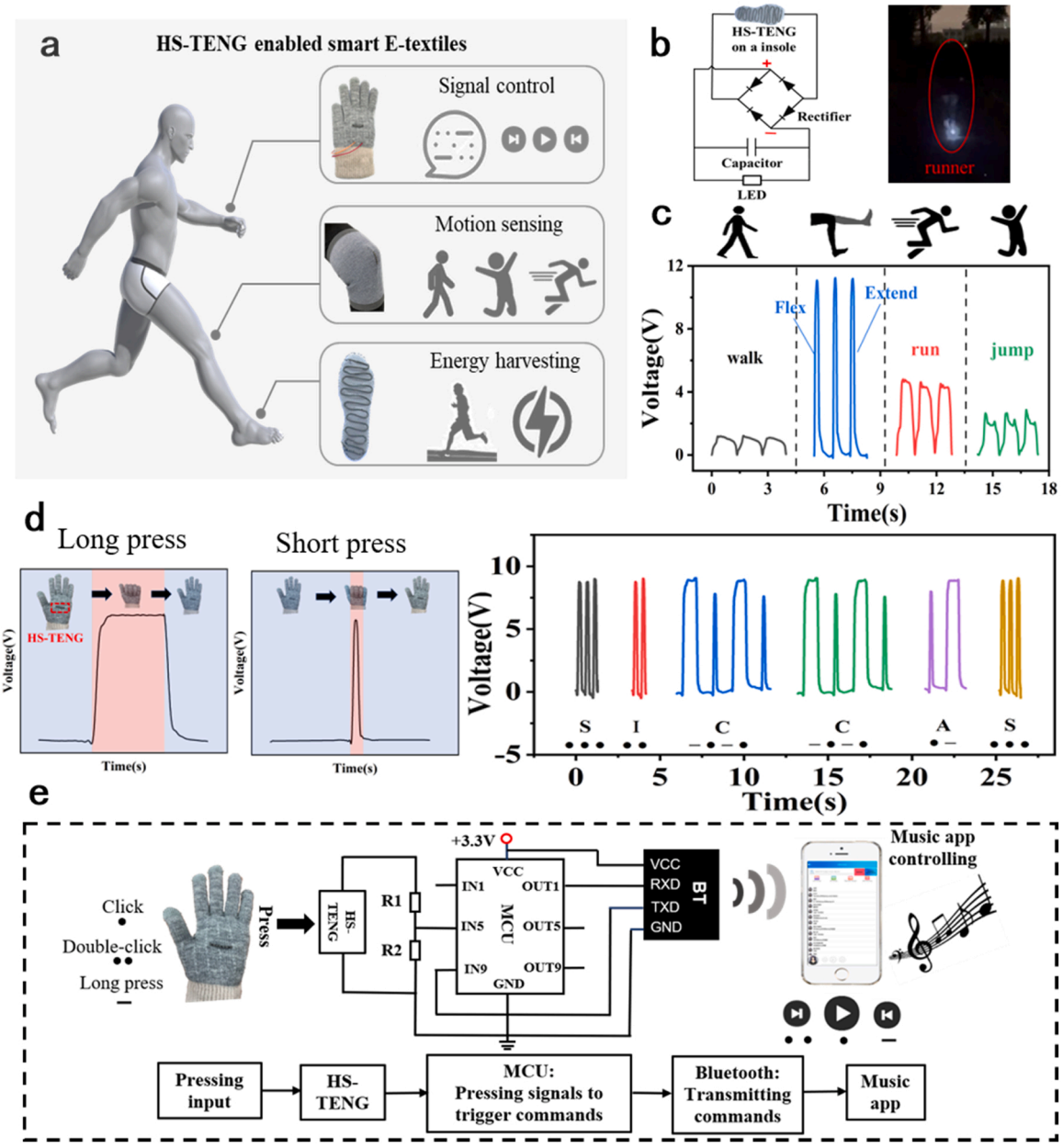

Fig. 5. HS-TENG enabled smart E-textiles for energy generation, sensing, and signal control. (a) Schematic illustration of the HS-TENG as wearable sensor integrated into various textiles, including insole for energy harvesting, kneepad for motion sensing, and glove for signal control. (b) The corresponding circuit diagram (left) and the image (right) of a runner equipped with HS-TENG based self-powered night-running warning system. (c) Voltage signals of the HS-TENG in response to walking, knee flexing/extending, running, and jumping. (d) Morse codes generated via pressing the HS-TENG, representing a phrase of "SICCAS". (e) Circuit diagram for signal control of music app on mobile phone.

bending can be effectively captured. As shown in Fig. 5c, the HS-TENG (sewn to the kneepad) records the electrical signals. It can discriminate various motions including knee flexing/extending, walking, running, and jumping, according to their distinctly differentiated waveforms. In addition to the strenuous knee-related exercise, some relatively gentle motions including finger bending, are also significant biomechanical information for healthcare or human-machine interaction applications. As shown in Fig. S18, the HS-TENG is attached on the index finger to achieve real-time voltage responses to finger bending. The outputs increase as the bending angles of the finger increase, which is attributed to the increasing effective contact area between the $Ti_3C_2T_x$ tribo-layer and Ecoflex. In addition, The HS-TENG also can be sewn on the palm of the glove (top of Fig. 5a). The voltage signals generated through long press and short press can be identified as "dash" or "dot" signals in sequences of Morse codes. Fig. 5d shows a series of V_{OC} signals created by pressing, representing a phrase of "SICCAS", achieving the conversion from pressing to useful information. Here, we further demonstrate the HS-TENG to serve as the wireless signal controller of the music app on mobile phone. Circuit diagram can be found in Fig. 5e, where the microcontroller unit (MCU) with the related circuit and Bluetooth module is used to process the signals. More specifically, a HS-TENG based haptic sensor generates an original press signal by pressing and rising trigger signals after rectification and smoothing. And then, different signal types are converted into different passwords by the MCU to trigger different commands, which are transmitted to the mobile phone through the Bluetooth module to realize the signal control of the music app (detailed information in Supplementary Note 3, Supporting information). Short press (That corresponds to a dot) controls "Play" or "Pause", double short press (That corresponds to two dots) controls "Next", and long press (That corresponds to a dash) controls "Previous" (Movie S3 in Supporting information). Due to the advantages of flexibility and easy integration, the smart glove has potential application prospects as a wearable tactile control system in many fields such as soft robots, automatic control, and smart home [63–65].

Supplementary material related to this article can be found online at doi:10.1016/j.nanoen.2022.107588.

3. Conclusion

In summary, a flexible and versatile helical-structured triboelectric nanogenerator (HS-TENG) is devised. The HS-TENG with high stretchability (~ 200 %) can produce high electrical outputs (52 V, 1.5 μA, 4.2 μW under 3 Hz, 2 cm long device), and can respond to multiple forms of mechanical stimuli (stretch, press, twist, bend) simultaneously. Furthermore, HS-TENG can be easily integrated into functional E-textiles for versatile applications, including energy harvesting, motion sensing, and wireless signal control. Our HS-TENG and the E-textiles could greatly promote the development of fiber electronics.

4. Experimental section

4.1. Materials

AgNWs(10 mg/mL, Zhejiang Kechuang New Materials Co., Ltd.), PEDOT: PSS (1 wt%, Xi'an Baolight Optoelectronics Technology Co., Ltd.), Ecoflex (Smooth-On, Inc., A and B components in the weight ratio of 1:1), HCl and LiF were purchased from Tansoole. PU fiber and copper wire were purchased from a local supermarket.

4.2. Preparation of $Ti_3C_2T_x$ /PEDOT: PSS and AgNW inks

2 g LiF powder was slowly immersed into 23 mL 9 M HCl to prepare the etchant. During the etching process, Ti_3AlC_2 (1 g) powder was treated with the etchant under continuous stirring for 48 h at 60 ℃. The resulting mixture was washed with distilled water and centrifuged until the pH was above 6. The precipitates were then collected by vacuum filtration and dried by vacuum freeze dryer, to obtain multilayer $Ti_3C_2T_x$ powder. Afterward, 1 g sediment was added into 50 mL distilled water, which was followed by 1 h sonication and 1 h centrifugation at 3500 rpm. The supernatant containing delaminated $Ti_3C_2T_x$ was achieved in the final step. Alternatively, we added PEDOT: PSS to the $Ti_3C_2T_x$ dispersion. The $Ti_3C_2T_x$ dispersion and PEDOT: PSS were mixed 2:1 by weight. Then the mixture was continually stirred for 12 h to get homogeneous $Ti_3C_2T_x$ /PEDOT: PSS ink. AgNWs were dispersed in isopropanol/water mixed solvent by bath sonication. Polyvinyl pyrrolidone (PVP) was added to facilitate the dispersion of AgNWs. The concentration of the AgNW ink is 10 mg/mL.

4.3. Fabrication of core fiber with AgNW/ $Ti_3C_2T_x$/ PEDOT: PSS coating

The PU/PET elastic fibers (≈ 600 μm, 3 mm in diameter) are commercially available. Firstly, the fibers were cleaned in ethanol with ultrasonic treatment for about 10 min and dried in air. Then the fibers were dip-coated in AgNW dispersion (10 mg/mL) for 5 s and immediately dried using a blow dryer. After this process was repeated several times, the AgNW-based fibers were dried at 80 ℃ in an oven for 20 min. The AgNW-based fiber was dip-coated in $Ti_3C_2T_x$ /PEDOT: PSS dispersion for specific times (5 s for each dip-coating) and dried in air. One end (defined as the electrode end of the fiber) was connected to a copper wire with the aid of silver paste for external circuit connection.

4.4. Fabrication of the sandwiched Ecoflex/AgNW-fabric/Ecoflex outer sheath

The commercial cotton elastic fabric was cut into ribbons as substrates. Firstly, the fabric was cleaned in ethanol with ultrasonic treatment for about 10 min and dried in air. Then the fabric was dip-coated in AgNW dispersion (10 mg/mL) for 5 s and immediately dried using a blow dryer. After this process was repeated several times, the AgNW-based fabric was dried at 80 ℃ in an oven for 20 min. The AgNW-based fabric was dipped into a liquid Ecoflex precursor from a 1A:1B mixture by weight leaving one end naked and then cured in an oven (80 ℃, 10 min). The end (defined as the electrode end of the fabric) was connected to a copper wire with the aid of silver paste for external circuit connection.

4.5. Assembly of the HS-TENG

The sandwiched Ecoflex/AgNW-fabric/Ecoflex outer sheath was helically wound around the core fiber to form a helically structured device. The helical turns and leaving gaps can be adjusted, copper wire as electrode lead is connected to both ends by conductive silver paint. The two ends of the device were fixed by the room temperature vulcanized silicone rubber.

4.6. Characterization and measurement

Hitachi SU4800 FE-SEM was used for scanning electron microscope (SEM) characterization. In the electromechanical performance test, the strain loading was carried out by a high-precision electric translation platform (Shanghai Weimu Optoelectronic Instrument Co., LTD., ZXT300MA06), and the real-time current signal was recorded by an electrochemical workstation (PARSTAT2273, Princeton Applied Research). In power generation performance tests, Linmot linear motors (E1100) are used to apply high-frequency stresses. Open circuit voltage, short circuit current, and transfer charge data were collected using a Keithley 6514 electrometer with a high-speed acquisition card. Concerning TENG simulation, COMSOL Multiphysics was used. In experiments involving human movement tests, individuals are thought to be electrically grounded. All electrical measurements were made at a relative humidity of 45 % and a temperature of 23 ℃. The surface potential of the tribo-materials were recorded using an electrostatic

voltmeter (Terk 542A).

CRediT authorship contribution statement

Fei Wu: Conceptualization, Methodology, Writing – original draft, Writing – review & editing. **Binxu Lan:** Data curation. **Yin Cheng:** Supervision. **Yi Zhou:** Software. **Gaffar Hossain:** Funding acquisition. **Günter Grabher:** Funding acquisition. **Liangjing Shi:** Resources. **Ranran Wang:** Project administration. **Jing Sun:** Resources.

Declaration of Competing Interest

The authors declare that they have no known competing financial interests or personal relationships that could have appeared to influence the work reported in this paper.

Data Availability

Data will be made available on request.

Acknowledgments

Financial support is gratefully acknowledged to the joint Project "POWERTEX-FFG/CAS: 875643/GJHZ2046" managed by Austrian Research Promotion Agency (FFG) and Chinese Academy of Sciences (CAS), National Natural Science Foundation of China (61871368, 62122080), Natural Science Foundation of Shanghai (22ZR1481700), and Shanghai Pujiang Program (21PJ1414800).

Appendix A. Supporting information

Supplementary data associated with this article can be found in the online version at doi:10.1016/j.nanoen.2022.107588.

References

[1] F. Wen, Z. Sun, T. He, Q. Shi, M. Zhu, Z. Zhang, L. Li, T. Zhang, C. Lee, Machine learning glove using self-powered conductive superhydrophobic triboelectric textile for gesture recognition in VR/AR applications, Adv. Sci. 7 (2020), 2000261.
[2] W. Gong, C. Hou, J. Zhou, Y. Guo, W. Zhang, Y. Li, Q. Zhang, H. Wang, Continuous and scalable manufacture of amphibious energy yarns and textiles, Nat. Commun. 10 (2019) 868.
[3] K. Dong, X. Peng, Z.L. Wang, Fiber/fabric-based piezoelectric and triboelectric nanogenerators for flexible/stretchable and wearable electronics and artificial intelligence, Adv. Mater. 32 (2020), e1902549.
[4] Z. Lou, L. Li, L. Wang, G. Shen, Recent progress of self-powered sensing systems for wearable electronics, Small 13 (2017).
[5] Y. Su, G. Chen, C. Chen, Q. Gong, G. Xie, M. Yao, H. Tai, Y. Jiang, J. Chen, Self-powered respiration monitoring enabled by a triboelectric nanogenerator, Adv. Mater. 33 (2021), e2101262.
[6] W. Fan, Q. He, K. Meng, X. Tan, Z. Zhou, G. Zhang, J. Yang, Z.L. Wang, Machine-knitted washable sensor array textile for precise epidermal physiological signal monitoring, Sci. Adv. 6 (2020) eaay2840.
[7] S.K. Karan, S. Maiti, J.H. Lee, Y.K. Mishra, B.B. Khatua, J.K. Kim, Recent advances in self-powered tribo-/piezoelectric energy harvesters: all-in-one package for future smart technologies, Adv. Funct. Mater. 30 (2020), 2004446.
[8] H. Yang, M. Wang, M. Deng, H. Guo, W. Zhang, H. Yang, Y. Xi, X. Li, C. Hu, Z. Wang, A full-packaged rolling triboelectric-electromagnetic hybrid nanogenerator for energy harvesting and building up self-powered wireless systems, Nano Energy 56 (2019) 300–306.
[9] J. Wang, J. He, L. Ma, Y. Yao, X. Zhu, L. Peng, X. Liu, K. Li, M. Qu, A humidity-resistant, stretchable and wearable textile-based triboelectric nanogenerator for mechanical energy harvesting and multifunctional self-powered haptic sensing, Chem. Eng. J. 423 (2021).
[10] Y. Hu, Z. Zheng, Progress in textile-based triboelectric nanogenerators for smart fabrics, Nano Energy 56 (2019) 16–24.
[11] Y.D. Horev, A. Maity, Y. Zheng, Y. Milyutin, M. Khatib, M. Yuan, R. Y. Suckeveriene, N. Tang, W. Wu, H. Haick, Stretchable and highly permeable nanofibrous sensors for detecting complex human body motion, Adv. Mater. 33 (2021), e2102488.
[12] C. Wu, J.H. Park, B. Koo, X. Chen, Z.L. Wang, T.W. Kim, Capsule triboelectric nanogenerators: toward optional 3D integration for high output and efficient energy harvesting from broadband-amplitude vibrations, ACS Nano 12 (2018) 9947–9957.
[13] Z. Cui, W. Wang, L. Guo, Z. Liu, P. Cai, Y. Cui, T. Wang, C. Wang, M. Zhu, Y. Zhou, W. Liu, Y. Zheng, G. Deng, C. Xu, X. Chen, Haptically quantifying Young's modulus of soft materials using a self-locked stretchable strain sensor, Adv. Mater. (2021), e2104078.
[14] H.-J. Park, S. Kim, J.H. Lee, H.T. Kim, W. Seung, Y. Son, T.Y. Kim, U. Khan, N.-M. Park, S.-W. Kim, Self-powered motion-driven triboelectric electroluminescence textile system, ACS Appl. Mater. Interfaces 11 (2019) 5200–5207.
[15] K. Dong, Z.L. Wang, Self-charging power textiles integrating energy harvesting triboelectric nanogenerators with energy storage batteries/supercapacitors, J. Semicond. 42 (2021).
[16] Z. Bai, Y. Xu, C. Lee, J. Guo, Autonomously adhesive, stretchable, and transparent solid-state polyionic triboelectric patch for wearable power source and tactile sensor, Adv. Funct. Mater. (2021).
[17] Z. Bai, Y. Xu, J. Li, J. Zhu, C. Gao, Y. Zhang, J. Wang, J. Guo, An eco-friendly porous nanocomposite fabric-based triboelectric nanogenerator for efficient energy harvesting and motion sensing, ACS Appl. Mater. Interfaces 12 (2020) 42880–42890.
[18] P. Zhang, W. Zhang, H. Zhang, A high-performance textile-based triboelectric nanogenerator manufactured by a novel brush method for self-powered human motion pattern detector, Sustain. Energy Technol. Assess. 46 (2021).
[19] H. Zhang, P. Zhang, W. Zhang, A high-output performance mortise and tenon structure triboelectric nanogenerator for human motion sensing, Nano Energy 84 (2021).
[20] W. Seung, H.-J. Yoon, T.Y. Kim, H. Ryu, J. Kim, J.-H. Lee, J.H. Lee, S. Kim, Y. K. Park, Y.J. Park, S.-W. Kim, Boosting power-generating performance of triboelectric nanogenerators via artificial control of ferroelectric polarization and dielectric properties, Adv. Energy Mater. 7 (2017).
[21] Y. Dong, S.S.K. Mallineni, K. Maleski, H. Behlow, V.N. Mochalin, A.M. Rao, Y. Gogotsi, R. Podila, Metallic MXenes: a new family of materials for flexible triboelectric nanogenerators, Nano Energy 44 (2018) 103–110.
[22] L. Yin, K.N. Kim, J. Lv, F. Tehrani, M. Lin, Z. Lin, J.M. Moon, J. Ma, J. Yu, S. Xu, J. Wang, A self-sustainable wearable multi-modular E-textile bioenergy microgrid system, Nat. Commun. 12 (2021) 1542.
[23] Y.-C. Lai, J. Deng, S.L. Zhang, S. Niu, H. Guo, Z.L. Wang, Single-thread-based wearable and highly stretchable triboelectric nanogenerators and their applications in cloth-based self-powered human-interactive and biomedical sensing, Adv. Funct. Mater. 27 (2017).
[24] W. Wang, J. Cao, J. Yu, R. Liu, C.R. Bowen, W.H. Liao, Self-powered smart insole for monitoring human gait signals, Sensors 19 (2019).
[25] W. Liu, Z. Wang, G. Wang, G. Liu, J. Chen, X. Pu, Y. Xi, X. Wang, H. Guo, C. Hu, Z. L. Wang, Integrated charge excitation triboelectric nanogenerator, Nat. Commun. 10 (2019) 1426.
[26] K. Dong, Y. Hu, J. Yang, S.-W. Kim, W. Hu, Z.L. Wang, Smart textile triboelectric nanogenerators: current status and perspectives, MRS Bull. 46 (2021) 512–521.
[27] C. Ning, K. Dong, R. Cheng, J. Yi, C. Ye, X. Peng, F. Sheng, Y. Jiang, Z.L. Wang, Flexible and stretchable fiber-shaped triboelectric nanogenerators for biomechanical monitoring and human-interactive sensing, Adv. Funct. Mater. 31 (2020).
[28] W. Ma, Y. Zhang, S. Pan, Y. Cheng, Z. Shao, H. Xiang, G. Chen, L. Zhu, W. Weng, H. Bai, M. Zhu, Smart fibers for energy conversion and storage, Chem. Soc. Rev. 50 (2021) 7009–7061.
[29] L. Lan, C. Jiang, Y. Yao, J. Ping, Y. Ying, A stretchable and conductive fiber for multifunctional sensing and energy harvesting, Nano Energy 84 (2021).
[30] D. Zhang, W. Yang, W. Gong, W. Ma, C. Hou, Y. Li, Q. Zhang, H. Wang, Abrasion resistant/waterproof stretchable triboelectric yarns based on fermat spirals, Adv. Mater. 33 (2021), e2100782.
[31] W.R. Cheng Y, K.H. Chan, X. Lu, J. Sun, G.W. Ho, A biomimetic conductive tendril for ultrastretchable and integratable electronics, muscles, and sensors, ACS Nano 12 (4) (2018) 3898–3907.
[32] K. Dong, Y.C. Wang, J. Deng, Y. Dai, S.L. Zhang, H. Zou, B. Gu, B. Sun, Z.L. Wang, A highly stretchable and washable all-yarn-based self-charging knitting power textile composed of fiber triboelectric nanogenerators and supercapacitors, ACS Nano 11 (2017) 9490–9499.
[33] C. Ning, R. Cheng, Y. Jiang, F. Sheng, J. Yi, S. Shen, Y. Zhang, X. Peng, K. Dong, Z. L. Wang, Helical fiber strain sensors based on triboelectric nanogenerators for self-powered human respiratory monitoring, ACS Nano 16 (2022) 2811–2821.
[34] J. Gao, Y. Fan, Q. Zhang, L. Luo, X. Hu, Y. Li, J. Song, H. Jiang, X. Gao, L. Zheng, W. Zhao, Z. Wang, W. Ai, Y. Wei, Q. Lu, M. Xu, Y. Wang, W. Song, X. Wang, W. Huang, Ultra-robust and extensible fibrous mechanical sensors for wearable smart healthcare, Adv. Mater. (2022), e2107511.
[35] K. Dong, J. Deng, W. Ding, A.C. Wang, P. Wang, C. Cheng, Y.-C. Wang, L. Jin, B. Gu, B. Sun, Z.L. Wang, Versatile core-sheath yarn for sustainable biomechanical energy harvesting and real-time human-interactive sensing, Adv. Energy Mater. 8 (2018).
[36] Y. Cheng, R. Wang, H. Zhai, J. Sun, Stretchable electronic skin based on silver nanowire composite fiber electrodes for sensing pressure, proximity, and multidirectional strain, Nanoscale 9 (2017) 3834–3842.
[37] C. Li, D. Liu, C. Xu, Z. Wang, S. Shu, Z. Sun, W. Tang, Z.L. Wang, Sensing of joint and spinal bending or stretching via a retractable and wearable badge reel, Nat. Commun. 12 (2021) 2950.
[38] X. He, Y. Zi, H. Guo, H. Zheng, Y. Xi, C. Wu, J. Wang, W. Zhang, C. Lu, Z.L. Wang, A highly stretchable fiber-based triboelectric nanogenerator for self-powered wearable electronics, Adv. Funct. Mater. 27 (2017).
[39] Y. Cheng, R. Wang, J. Sun, L. Gao, Highly conductive and ultrastretchable electric circuits from covered yarns and silver nanowires, ACS Nano 9 (2015) 3887–3895.

[40] X. Hu, M. Tian, T. Xu, X. Sun, B. Sun, C. Sun, X. Liu, X. Zhang, L. Qu, Multiscale disordered porous fibers for self-sensing and self-cooling integrated smart sportswear, ACS Nano 14 (2020) 559–567.
[41] W. Gong, C. Hou, Y. Guo, J. Zhou, J. Mu, Y. Li, Q. Zhang, H. Wang, A wearable, fibroid, self-powered active kinematic sensor based on stretchable sheath-core structural triboelectric fibers, Nano Energy 39 (2017) 673–683.
[42] Z. Feng, S. Yang, S. Jia, Y. Zhang, S. Jiang, L. Yu, R. Li, G. Song, A. Wang, T. Martin, L. Zuo, X. Jia, Scalable, washable and lightweight triboelectric-energy-generating fibers by the thermal drawing process for industrial loom weaving, Nano Energy 74 (2020).
[43] B. Chen, Y. Yang, Z.L. Wang, Scavenging wind energy by triboelectric nanogenerators, Adv. Energy Mater. 8 (2018).
[44] J. Han, C. Xu, J. Zhang, N. Xu, Y. Xiong, X. Cao, Y. Liang, L. Zheng, J. Sun, J. Zhai, Q. Sun, Z.L. Wang, Multifunctional coaxial energy fiber toward energy harvesting, storage, and utilization, ACS Nano 15 (2021) 1597–1607.
[45] R. Zhang, C. Dahlstrom, H. Zou, J. Jonzon, M. Hummelgard, J. Ortegren, N. Blomquist, Y. Yang, H. Andersson, M. Olsen, M. Norgren, H. Olin, Z.L. Wang, Cellulose-based fully green triboelectric nanogenerators with output power density of 300 W m^{-2}, Adv. Mater. 32 (2020), e2002824.
[46] Y.C. Lai, H.W. Lu, H.M. Wu, D. Zhang, J. Yang, J. Ma, M. Shamsi, V. Vallem, M. D. Dickey, Elastic multifunctional liquid–metal fibers for harvesting mechanical and electromagnetic energy and as self-powered sensors, Adv. Energy Mater. 11 (2021).
[47] X. Zhang, Z. Li, W. Du, Y. Zhao, W. Wang, L. Pang, L. Chen, A. Yu, J. Zhai, Self-powered triboelectric-mechanoluminescent electronic skin for detecting and differentiating multiple mechanical stimuli, Nano Energy 96 (2022).
[48] Y. Cheng, R. Wang, J. Sun, L. Gao, A stretchable and highly sensitive graphene-based fiber for sensing tensile strain, bending, and torsion, Adv. Mater. 27 (2015) 7365–7371.
[49] L. Huang, S. Lin, Z. Xu, H. Zhou, J. Duan, B. Hu, J. Zhou, Fiber-based energy conversion devices for human-body energy harvesting, Adv. Mater. 32 (2020), e1902034.
[50] J. Ge, L. Sun, F.R. Zhang, Y. Zhang, L.A. Shi, H.Y. Zhao, H.W. Zhu, H.L. Jiang, S. H. Yu, A stretchable electronic fabric artificial skin with pressure-, lateral strain-, and flexion-sensitive properties, Adv. Mater. 28 (2016) 722–728.
[51] K. Fu, J. Zhou, H. Wu, Z. Su, Fibrous self-powered sensor with high stretchability for physiological information monitoring, Nano Energy 88 (2021).
[52] Y. Cheng, X. Lu, K. Hoe Chan, R. Wang, Z. Cao, J. Sun, G. Wei Ho, A stretchable fiber nanogenerator for versatile mechanical energy harvesting and self-powered full-range personal healthcare monitoring, Nano Energy 41 (2017) 511–518.
[53] H. Wu, Z. Wang, Y. Zi, Multi-mode water-tube-based triboelectric nanogenerator designed for low-frequency energy harvesting with ultrahigh volumetric charge density, Adv. Energy Mater. 11 (2021).
[54] K. Dong, X. Peng, R. Cheng, Z.L. Wang, Smart textile triboelectric nanogenerators: prospective strategies for improving electricity output performance, Nanoenergy Adv. 2 (2022) 133–164.
[55] K. Dong, X. Peng, R. Cheng, C. Ning, Y. Jiang, Y. Zhang, Z.L. Wang, Advances in high-performance autonomous energy and self-powered sensing textiles with novel 3D fabric structures, Adv. Mater. (2022), e2109355.
[56] Y. Yang, L. Shi, Z. Cao, R. Wang, J. Sun, Strain sensors with a high sensitivity and a wide sensing range based on a Ti3C2Tx(MXene) nanoparticle–nanosheet hybrid network, Adv. Funct. Mater. 29 (2019).
[57] M. Salauddin, S.M.S. Rana, M.T. Rahman, M. Sharifuzzaman, P. Maharjan, T. Bhatta, H. Cho, S.H. Lee, C. Park, K. Shrestha, S. Sharma, J.Y. Park, Fabric-assisted MXene/silicone nanocomposite-based triboelectric nanogenerators for self-powered sensors and wearable electronics, Adv. Funct. Mater., 2021.
[58] K. Shrestha, S. Sharma, G.B. Pradhan, T. Bhatta, P. Maharjan, S.M.S. Rana, S. Lee, S. Seonu, Y. Shin, J.Y. Park, A siloxene/Ecoflex nanocomposite-based triboelectric nanogenerator with enhanced charge retention by MoS_2/LIG for self-powered touchless sensor applications, Adv. Funct. Mater., 2022.
[59] Y. Jiang, K. Dong, X. Li, J. An, D. Wu, X. Peng, J. Yi, C. Ning, R. Cheng, P. Yu, Z.L. Wang, Stretchable, washable, and ultrathin triboelectric nanogenerators as skin-like highly sensitive self-powered haptic sensors, vol. 31, 2021, 2005584.
[60] J.-H. Pu, X. Zhao, X.-J. Zha, W.-D. Li, K. Ke, R.-Y. Bao, Z.-Y. Liu, M.-B. Yang, W. Yang, A strain localization directed crack control strategy for designing MXene-based customizable sensitivity and sensing range strain sensors for full-range human motion monitoring, Nano Energy 74 (2020), 104814.
[61] Q. Zhang, T. Jin, J. Cai, L. Xu, T. He, T. Wang, Y. Tian, L. Li, Y. Peng, C. Lee, Wearable triboelectric sensors enabled gait analysis and waist motion capture for IoT-based smart healthcare applications, Adv. Sci. (2021), e2103694.
[62] M. He, W. Du, Y. Feng, S. Li, W. Wang, X. Zhang, A. Yu, L. Wan, J. Zhai, Flexible and stretchable triboelectric nanogenerator fabric for biomechanical energy harvesting and self-powered dual-mode human motion monitoring, Nano Energy 86 (2021).
[63] Z. Zhang, T. He, M. Zhu, Z. Sun, Q. Shi, J. Zhu, B. Dong, M.R. Yuce, C. Lee, Deep learning-enabled triboelectric smart socks for IoT-based gait analysis and VR applications, npj Flex. Electron. 4 (2020).
[64] Z. Yan, L. Wang, Y. Xia, R. Qiu, W. Liu, M. Wu, Y. Zhu, S. Zhu, C. Jia, M. Zhu, R. Cao, Z. Li, X. Wang, Flexible high-resolution triboelectric sensor array based on patterned laser-induced graphene for self-powered real-time tactile sensing, Adv. Funct. Mater. 31 (2021).
[65] X. Yang, G. Liu, Q. Guo, H. Wen, R. Huang, X. Meng, J. Duan, Q. Tang, Triboelectric sensor array for internet of things based smart traffic monitoring and management system, Nano Energy 92 (2022).

Wu Fei received her B.S. degree (2020) in materials science and engineering from Qingdao University of Technology and now is a MA. Eng candidate in Shanghai Institute of Ceramics, Chinese Academy of Sciences (SICCAS) in Prof. Sun Jing's group. Her research interests include fiber sensors for wearable electronics.

Lan Binxu received his master's degree from Hubei University of Technology in 2020. He is currently a research assistant in Shanghai Institute of Ceramics, Chinese Academy of Sciences, His research interests include flexible sensors and flexible energy storage devices.

Cheng Yin received the B.S. degree (2011) in materials science and engineering from North China Electric Power University (Beijing) and the Ph.D. degree (2016) in Materials Physics and Chemistry from Shanghai Institute of Ceramics, Chinese Academy of Sciences (SICCAS). He is now working as an associate Professor in SICCAS, focusing on flexible and wearable electronics.

Zhou Yi received his B.Eng. degree (2017) in Nuclear Engineering and Technology from Lanzhou University and M.Sc. degree (2019) in Physics from Harbin Institute of Technology. He is now a Ph.D. candidate at Electrical and Computer Engineering, National University of Singapore. His research interests include photothermal management and energy harvesting, radioisotope power systems (RPS), hybrid energy systems, novel power technology and conversion.

Gaffar Hossain received his European doctorate degree in polymer and biopolymer in 2011 from the Technical University of catalonia, Barcelona, Spain. In 2005 he has ended his Masters in Textile engineering and Technology from Dresden University of Technical, Germany. From 2011 up to now he is acting as the research leader and head of the Institute V-Trion GmbH textile research in Austria.

Günter Grabher completed his diploma in textile technology from Höhere Technische Lehranstalt (HTL), Dornbirn (Austria) in 1990. He gained over 30 years of his experience in the field of textile finishing, embroidery, knitting, finishing, technical textile as well as in smart textile. He is currently the founder of Grabher Group.

Shi Liangjing received his B.S. degree from Shanghai Jiaotong University and Ph.D. degree (2013) from SICCAS. He is now working as an assistant researcher in SICCAS. His research interests include preparation and application of CVD graphene and controllable synthesis and industrialization of metal nanowires and their applications.

Wang Ranran received her B.S. degree (2007) from China University of Petroleum and Ph.D. degree (2012) from SICCAS. She is now working as a Professor in SICCAS. Her research interests include low dimensional conductive materials, stretchable electrodes and conductors, flexible and wearable sensors.

Sun Jing received her M.S. from Changchun Institute of Applied Chemistry and Ph.D. degree from Shanghai Institute of Ceramics in 1994 and 1997, respectively. Then she joined Shanghai Institute of Ceramics (SICCAS). She spent one year as visiting scientist in Institute for Surface Chemistry in Stockholm (YKI) between 1999 and 2000 and as a JSPS fellow in National Institute of Advanced Science and Technology (AIST) in Japan during 2002–2004. She has been appointed as a Professor in SICCAS since 2005 and now is leading a research group focusing on photo-catalysis for indoors & outdoors air-cleaning and flexible electronics.